Supporting information

Peroxidase-like Activity of Hollow Sphere-like FeS_2/SC Boosted by Synergistic Action of Defects and S-C Bonding

Hao Tan and Zhaodong Nan

Table S1. Mass fraction of FeS_2 loading in FeS_2/SC determined by ICP-AES.

FeS_2/SC	FeS_2/SC (mg/L)	Fe amount (mg/L)	Mass fraction of FeS_2 (%)
FeS_2/SC-2.5%	1000	453.8	97.5
FeS_2/SC-5.0%	1000	442.2	95.0
FeS_2/SC-5.3%	1000	440.8	94.7
FeS_2/SC-7.5%	1000	430.5	92.5
FeS_2/SC-10.0%	1000	418.9	90.0
FeS_2/SC-12.5%	1000	407.3	87.5

Response Surface Methodology (RSM). The experimental temperature was fixed at 25 ℃, the concentrations of H_2O_2 and TMB were 60 μM and 1.2 mM, respectively, and the reaction time was 1 min. Response Surface Methodology (RSM) based on BBD (Box-Behnken Design) was used to optimize the experimental conditions. A second-order polynomial equation was obtained as the following,

$$y = 2.05 - 0.425X_1 + 0.0737X_2 + 0.0613X_3 - 0.0175X_1X_2 + 0.0075X_1X_3 - 0.02X_2X_3 - 0.796{X_1}^2 - 0.1785{X_2}^2 - 0.2185{X_3}^2 \quad (1)$$

where X_1, X_2, and X_3 present solution pH, nanozymic concentration (μg/mL), and the content of the carbon in FeS_2/SC (wt%), y is the absorbance value of the solution at 652 nm (A_{652nm}). The reaction conditions were obtained according to the maximum value of y.

The values of X_1, X_2, and X_3 were selected as listed in Table S2. For example, the experimental result indicated that A_{652nm} reached the highest at pH = 4.0 among pH values (3.5, 4.0, 4.5, 5.0, 5.5, and 6.0). Thus, X_1 was selected as 3.5, 4.0, and 4.5. Table S2 lists the results (A_{652nm}) obtained through the experiment and the calculated based on Eq. (1), indicating that Eq. (1) can be used as a model to predict the experimental result. The individual and mutual effects between y and X (X_1, X_2, and X_3) were studied by two-dimensional (2D) contour lines and three-dimensional (3D) surface maps. All 2D contour lines were elliptic contour lines in Figures S1A and D, indicating that the interaction was significant.[1] Figures S1B and E show the interaction between pH and the content of the carbon in FeS_2/SC. Figures S1C and F reflect the effect of nanozymic concentration and the content of the carbon in FeS_2/SC. The optimized conditions were obtained as pH 3.83, naozymic concentration 255 μg/mL, and the content of the carbon in FeS_2/SC 5.31 wt%.

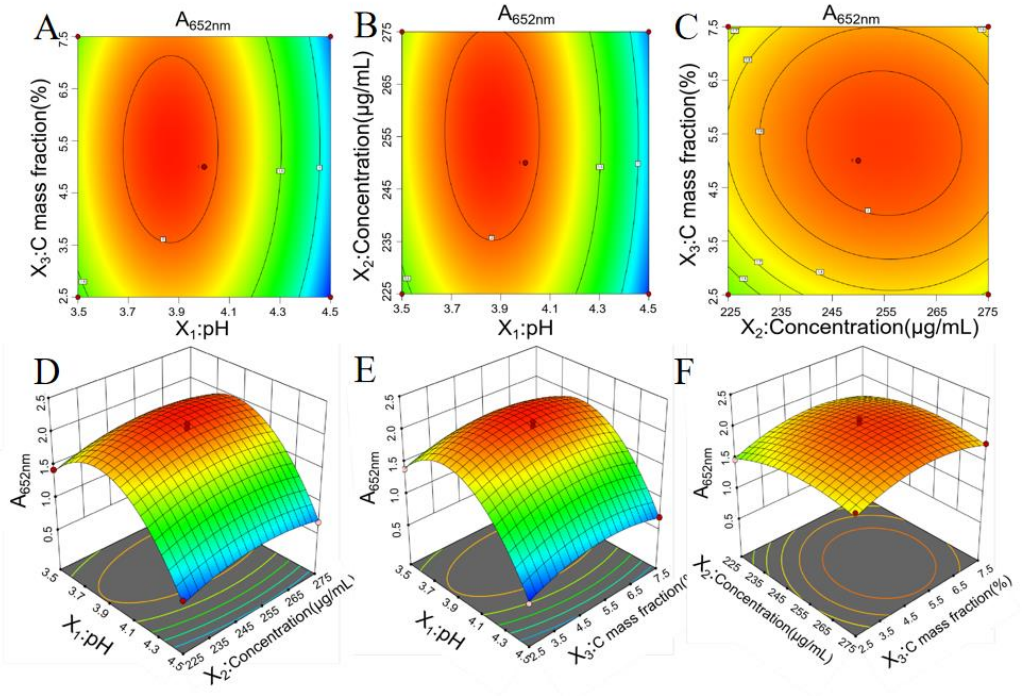

Figure S1. 2D contour diagram and 3D surface diagram of the influence of various factors on POD activity (A_{652}), (A) and (D) X_1 and X_2 (X_3 = 5.0), (B) and (E) X_1 and X_3 (X_2 = 250), (C) and (F) X_2 and X_3 (X_1 = 4.0).

Table S2. Experimental and calculated results based on Eq. (1).

Run	X_1	X_2 (μg/mL)	X_3 (wt%)	y	
				Experimental	calculated
1	3.5	225	5.0	1.44	1.41
2	4.5	225	5.0	0.65	0.60
3	3.5	275	5.0	1.54	1.59
4	4.5	275	5.0	0.68	0.71
5	3.5	250	2.5	1.40	1.41
6	4.5	250	2.5	0.51	0.54
7	3.5	250	7.5	1.55	1.52
8	4.5	250	7.5	0.69	0.68
9	4.0	225	2.5	1.48	1.50
10	4.0	275	2.5	1.75	1.69
11	4.0	225	7.5	1.6	1.66
12	4.0	275	7.5	1.79	1.77
13	4.0	250	5.0	1.97	2.05
14	4.0	250	5.0	2.01	2.05
15	4.0	250	5.0	2.10	2.05
16	4.0	250	5.0	2.05	2.05
17	4.0	250	5.0	2.08	2.05

In order to further evaluate the adequacy and significance of the model, a linear graph was obtained with a good correlation (R^2 = 0.9916) and a slope of 0.99213 between the predicted value of the model and the experimental value as shown in Figure S2, indicating that the model fit was significant. In addition, the residual distribution diagram is also an important factor to evaluate whether the model fitting results are significant in Figure. S3,[2] which fits well with the straight line, indicating no serious non-normality.[3] It can be seen in Figure. S4 that the residual was distributed between -3.0 and +3.0. The results prove that the model well represents the relationship between A_{652nm} (y) and independent variables (X_1, X_2, and X_3).[3] ANOVA analysis was performed on the model as given in Table S3. F-value was 98.05 and P-value >0.0001, indicating that the model was significant. The comparison of F-values of each variable factor can reflect the influence on the dependent variable (A_{652nm}).[4] The results show that the influence capacity of A_{652nm} is $X_1 > X_2 > X_3$. "Lack of Fit F-value" is 1.30, indicating that "Lack of Fit" is not significant compared with the pure error. The second-order polynomial model coefficient (R^2) and adjustment coefficient (Adjust R^2) are 0.9921 and 0.9820, indicating that the model response value is in good agreement with the experimental value.[5] The variance coefficient (C.V.%) is 4.90, indicating that the model has high accuracy and reliability.[6.]

Table S3 ANOVA for $A_{652\ nm}$ from BBD.

Source	Sum of Squares	df	Mean Square	F-value	p-value	
Model	4.71	9	0.5233	98.05	< 0.0001	significant
X_1	1.44	1	1.44	270.78	< 0.0001	
X_2	0.0435	1	0.0435	8.15	0.0245	
X_3	0.0300	1	0.0300	5.62	0.0495	
X_1X_2	0.0012	1	0.0012	0.2296	0.6465	
X_1X_3	0.0002	1	0.0002	0.0422	0.8432	
X_2X_3	0.0016	1	0.0016	0.2998	0.6010	
X_1^2	2.67	1	2.67	499.93	< 0.0001	
X_2^2	0.1342	1	0.1342	25.14	0.0015	
X_3^2	0.2010	1	0. 2010	37.67	0.0005	
Residual	0.0374	7	0.0053			
Lack of Fit	0.0185	3	0.0062	1.30	0.3885	not significant
Pure Error	0.0189	4	0.0047		.	
Cor Total	4.75	16				
Std. Dev.	0.0731		R^2	0.9921		
Mean	1.49		Adjusted R^2	0.9820		
C.V. %	4.90		Predicted R^2	0.9315		
			Adeq Precision	26.9198		

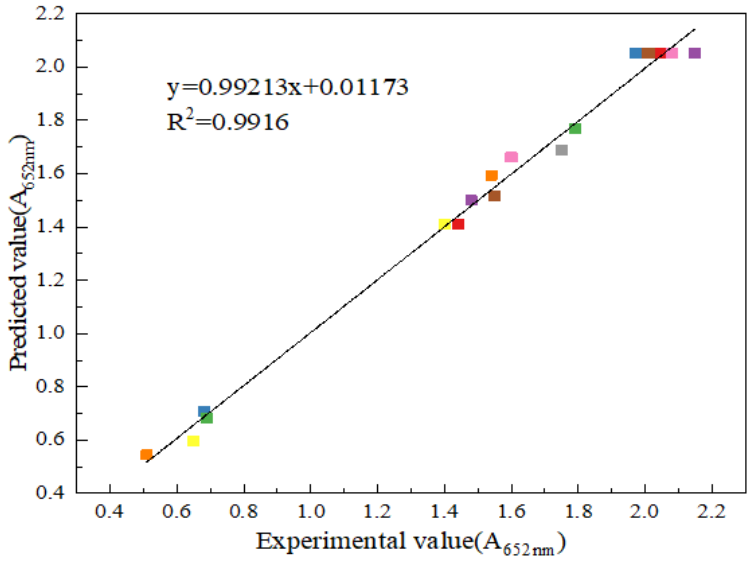

Figure S2. Predicted and experimental values of A_{652nm}.

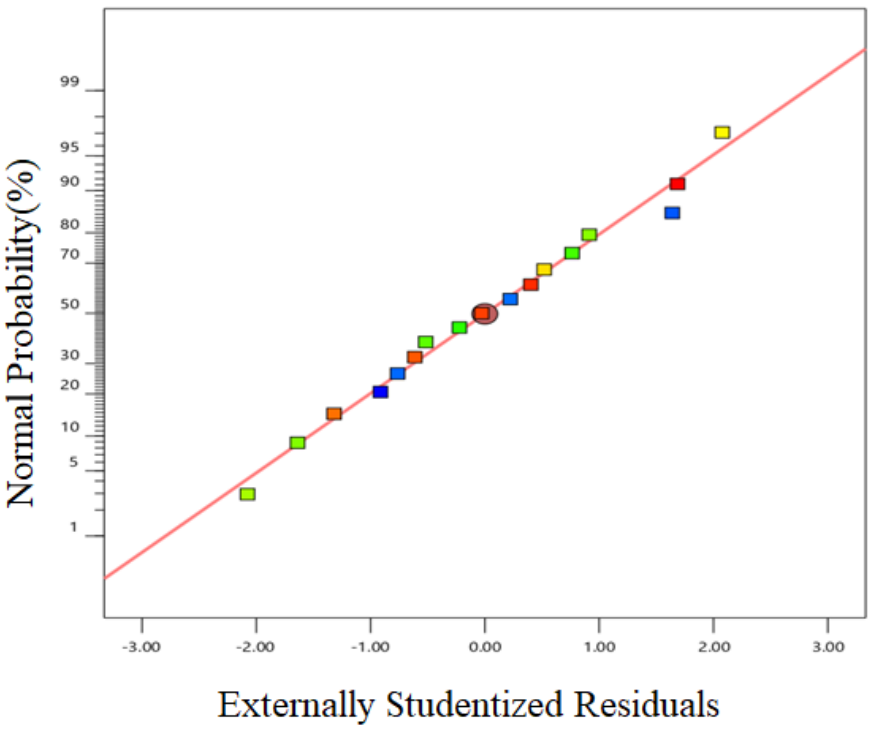

Figure S3. Normal probability plot of the internally studentized residuals for A_{652nm}.

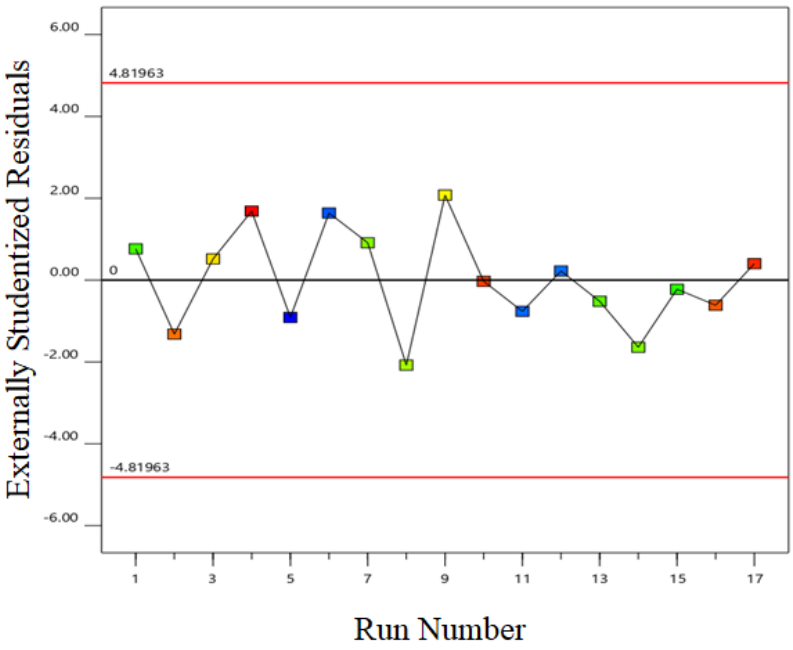

Figure S4 The run number versus residual data for A_{652nm}.

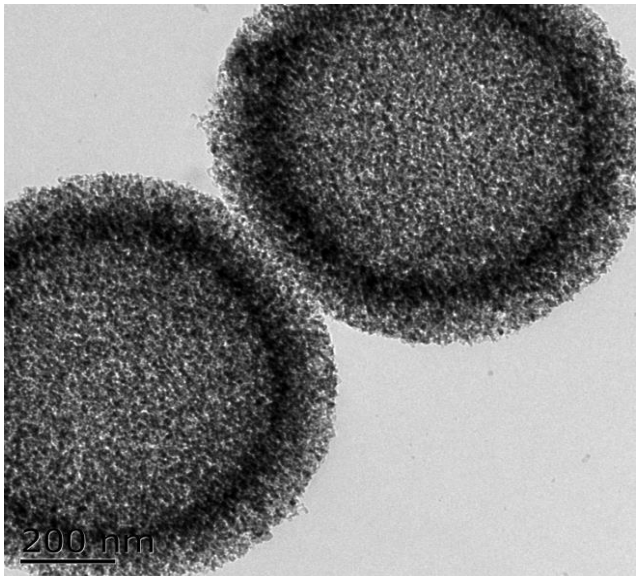

Figure S5. A TEM image of the hollow sphere-shaped carbon.

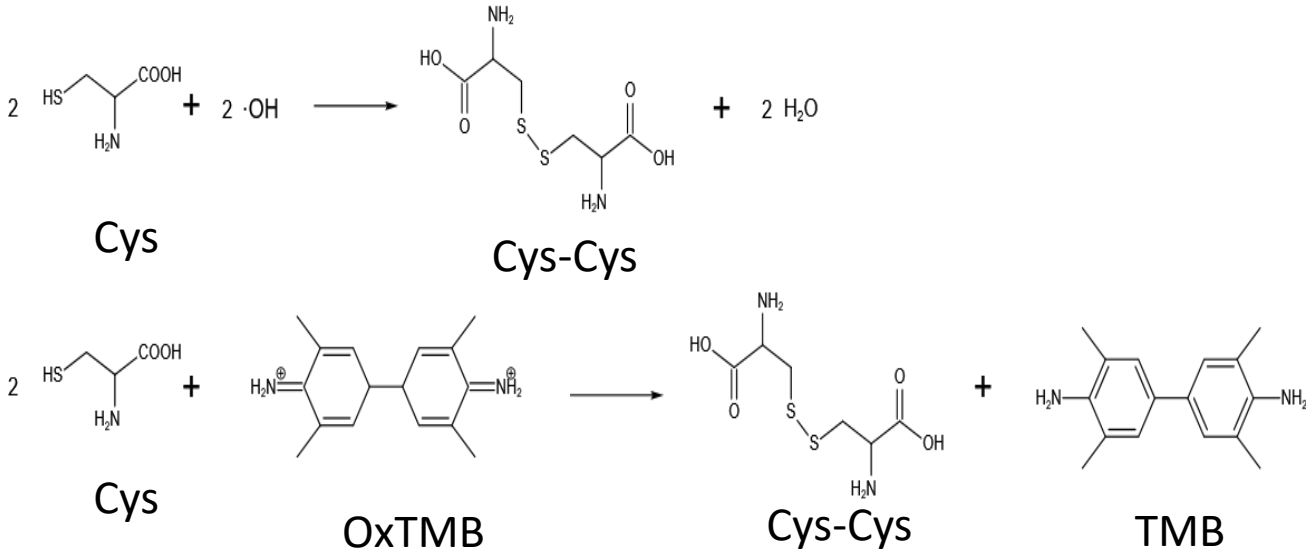

Figure S6. Mechanism of inhibiting oxidation of TMB by Cys.

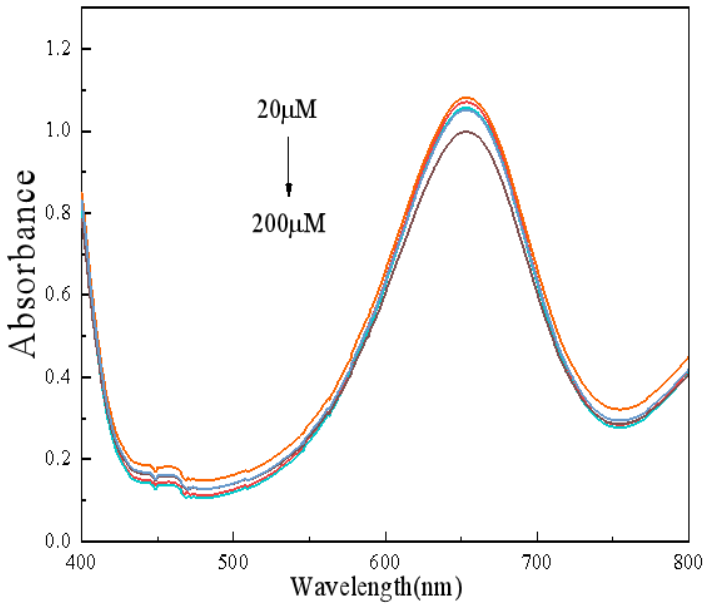

Figure S7. UV−vis absorbance spectra with different Cys concentrations from 20 to 200 μM with FeS_2/SiO_2 as the nanozyme.

REFERENCES

[1] Xin, S.; Liu, G.; Ma, X.; Gong, J.; Ma, B.; Yan, Q.; Chen, Q.; Ma, D.; Zhang, G.; Gao, M.; Xin, Y. High Efficiency Heterogeneous Fenton-like Catalyst Biochar Modified $CuFeO_2$ for the Degradation of Tetracycline: Economical Synthesis, Catalytic Performance and Mechanism. *Appl. Catal. B Environ*. **2021**, *280*, 119386.

[2] Chen, J.; Li, G.; Huang, Y.; Zhang, H.; Zhao, H.; An, T. Optimization Synthesis of Carbon Nanotubes-Anatase TiO_2 Composite Photocatalyst by Response Surface Methodology for Photocatalytic Degradation of Gaseous Styrene. *Appl. Catal. B Environ*. **2012**, *123 – 124*, 69 – 77.

[3] Hazime, R.; Nguyen, Q. H.; Ferronato, C.; Huynh, T. K. X.; Jaber, F.; Chovelon, J. M. Optimization of Imazalil Removal in the System UV/TiO_2/$K_2S_2O_8$ Using a Response Surface Methodology (RSM). *Appl. Catal. B Environ*. **2013**, *132 – 133*, 519 – 526.

[4] Xu, J.; Xing, Y.; Liu, Y.; Liu, M.; Hou, X. Facile in Situ Microwave Synthesis of Fe_3O_4@MIL-100(Fe) Exhibiting Enhanced Dual Enzyme Mimetic Activities for Colorimetric Glutathione Sensing. *Anal. Chim. Acta* **2021**, *1179*, 338825.

[5] Wang, M.; Zhang, B.; Cai, C.; Xin, Y.; Liu, H. Acidic Hydrothermal Treatment: Characteristics of Organic, Nitrogen and Phosphorus Releasing and Process Optimization on Lincomycin Removal from Lincomycin Mycelial Residues. *Chem. Eng. J*. **2018**, *336*, 436 – 444.

[6] Sulaiman, N. F.; Wan Abu Bakar, W. A.; Toemen, S.; Kamal, N. M.; Nadarajan, R. In Depth Investigation of Bi-Functional, Cu/Zn/γ-Al2O3 Catalyst in Biodiesel Production from Low-Grade Cooking Oil: Optimization Using Response Surface Methodology. *Renew. Energy* **2019**, *135*, 408–416.